

Oxygen electroreduction on polycrystalline gold electrodes and on gold nanoparticle-modified glassy carbon electrodes

Chinnaya Jeyabharathi · Ulrich Hasse · Paula Ahrens · Fritz Scholz

Received: 19 September 2014 / Revised: 8 October 2014 / Accepted: 8 October 2014 / Published online: 26 October 2014
© Springer-Verlag Berlin Heidelberg 2014

Abstract The oxygen reduction reaction (ORR) in acid media can be catalyzed on gold electrodes when the surface is activated by mechanical or electrochemical pretreatments. The activation is caused by increased surface roughness and defects, or asperities. After activation, a slow recrystallization of the surface as a function of relaxation time leads to deactivation of the surface for the ORR. After removal of active centers, the surface is not affected over time, which reveals that the surface recrystallization is associated with the deactivation. Experiments using various amounts of Au nanoparticles (AuNPs) immobilized on glassy carbon (GC) show a positive shift of peak potential of oxygen reduction and peroxide oxidation with increasing particle coverage.

Keywords Oxygen reduction reaction · Electrocatalysis · Gold · Activation · Deactivation

Introduction

The oxygen reduction reaction (ORR) belongs to the most intensively studied electrochemical reactions [1–3]. The activity of the electrode can be enhanced or decreased, depending on protocols used to prepare the electrodes. There are many reports about the *activation* of metal substrates and the creation of active sites on Au and Pt, using different methods, viz., thermal pre-treatment [4–6], cathodic polarization [7, 8], potential cycling [9, 10], etc. Those active sites are

catalytically active in several electrochemical reactions. In a preceding paper, we have shown that the electrocatalytic activity of mechanically polished polycrystalline gold (pc-Au) electrodes can be *decreased* by treating the electrode surface with hydroxyl radicals [11], a process which goes along with the dissolution of the asperities and smoothing of the surface. It is understood that the asperities are required in catalyzing the oxygen reduction reaction, and their dissolution leads to the deactivation of the electrode for the reason that the gold atoms located on the asperities stabilize the free radical intermediates and hence lead to a higher catalytic activity. Here, we report experiments in which pc-Au was activated by mechanical polishing and also by electrochemical treatment. It was observed that the electrodes activated with respect to the ORR are deactivated over time, possibly as a result of relaxation processes of the surface. This deactivation of the electrodes on a time scale of hours has been followed by atomic force microscopy (AFM) at identical locations. Dissolution of the surface layer of pc-Au electrodes with KCN/O₂ solutions resulted in an extremely effective deactivation. As a model system for pc-Au electrodes with their electrocatalytic active asperities, the ORR was studied also on glassy carbon (GC) electrodes with increasing loads of Au nanoparticles (AuNPs). In all these cases, it was observed that activation has only a small effect on the size of the catalytic current, but strongly affects the signal position on the potential scale. Jena and Raj have shown that the shift of peak potential of the ORR with coverage of gold particles can be attributed to changes in the diffusion regime from mixed spherical to linear diffusion [12]. Compton et al. [13, 14] have simulated the electrocatalytic response of nanoparticle-covered electrodes and introduced the seminal idea of a coverage-dependent apparent rate constant. The experiments presented in this study are phenomenologically in complete agreement with Compton's simulation. These authors arrived at the coverage-dependent apparent rate constant from a theoretical analysis of a one-

The authors dedicate this paper to Stephen Fletcher on the occasion of his 65th birthday. FS would like to acknowledge Stephen's readiness to discuss at any time electrochemical problems, historical views, as well as the subtleties of the English language.

C. Jeyabharathi (✉) · U. Hasse · P. Ahrens · F. Scholz
Institute of Biochemistry, University of Greifswald,
Felix-Hausdorff-Str.4, 17487 Greifswald, Germany
e-mail: chinnayaj@uni-greifswald.de

electron irreversible electrode reaction proceeding at a *partially active, non-planar* electrode. Although this theory completely describes the experimentally observed behavior, it cannot be excluded that there is a real increase in rate constants caused by an increased clustering of nanoparticles with increasing coverage due to the effect of overlap of the electrical double layers of individual nanoparticles, as recently suggested by Nesselberger et al. [15].

Experimental

A three-electrode cell connected to an Autolab potentiostat (Metrohm AG) was used for the electrochemical experiments. Polycrystalline gold (pc-Au) electrodes of different origin were used as working electrodes (e.g., Metrohm electrodes, and homemade electrodes from Au plates and ingots) without detecting any difference. The gold or glassy carbon (GC) electrodes were polished using 1, 0.3, and 0.05 μm Al_2O_3 slurries on a velvet polishing pad (from Micropolish II, Buehler, USA) successively, cleaned well with Millipore water, sonicated, and finally rinsed with Millipore water. A glassy carbon rod was used as counter electrode, and an Ag/AgCl (3 M KCl) electrode from Metrohm AG as a reference ($E=0.210$ V vs SHE). The electrolyte and the reference electrolyte were separated by KNO_3 -agar salt bridges (polyethylene tubing filled with the salt-gel). For oxygen reduction reaction, oxygen-saturated 0.1 M H_2SO_4 (98 % H_2SO_4 , Emsure[®], for analysis, Merck) solutions were used with an oxygen-blanket maintained throughout the measurement. All the solutions were prepared using Millipore water with the resistivity of 18.2 $\text{M}\Omega$ cm (Sartorius arium[®] 611UV, Sartorius AG, Germany), and the temperature was maintained at 25 °C. Although the ORR curve is not a true wave, we denoted the half-peak potential of ORR as $E_{1/2}$ for convenience.

A gold nanoparticle sol was prepared by thermal citrate reduction: AuNPs were synthesized by taking an aqueous solution of 1.9 mM HAuCl_4 (prepared by dissolving gold; the concentration of HAuCl_4 was determined by using an Inductively Coupled Plasma Optical Emission Spectrometer (Optima 2100 DV, Perkin Elmer, USA); standard HAuCl_4 solution (CertiPUR[®]) from Merck KGaA, Germany was used for a comparison) and 3.8 mM trisodium citrate (extra pure) (VEB Laborchemie Apolda) in a total volume of 10 ml. Initially, the HAuCl_4 in water was heated to boiling while stirring the solution constantly with a magnetic stirrer. Then, the sodium citrate solution was added to the hot solution. The typical transformation of the solution to purple initially and later to wine-red was observed. The total volume of the sol was maintained constant by adding Millipore water during heating. UV-visible spectrum of the Au sol was recorded using a spectrometer Specord 50 (Analytik Jena, Germany).

The surface plasmon resonance (SPR) band (spectrum is not shown) at 524 nm is observed, which is typical of a gold sol with NPs of 17 to 20 nm diameter stabilized by citrate ions in water [16]. The average particle size determined by dynamic light scattering method using a Zetasizer (DTS Ver.5.10, Malvern Instruments) was 22 ± 1 nm. The AuNPs were drop cast on the surface of the glassy carbon electrode, dried overnight, and used for ORR measurement. SEM-energy dispersive X-ray (EDX) mapping of gold nanoparticles was done by a field emission scanning electron microscope of Zeiss (Zeiss Auriga-Carl Zeiss NTS Ltd) coupled with an energy dispersive X-ray spectrometer (X-Max[®]-Oxford Instruments).

Results and discussion

(A) Oxygen reduction on pc-Au electrodes

The surface of pc-Au electrodes can be activated by introducing energy to the surface by mechanical polishing with the help of wet abrasive alumina powder on a polishing pad. Figure 1 shows the cyclic voltammograms (CVs) of the as-polished gold electrode and the same electrode after several electrochemical cycles with their respective responses to the ORR. The CVs in Fig. 1a show gold oxidation in the forward scan and the reduction of the gold oxide in the reverse scan. After 50 to 150 potential cycles, the shape of the CV is very reproducible and exhibits the typical splitting of the anodic peak into three small peaks and a sharp reduction peak with a rather large Faradaic capacity. The electrochemical pretreatment can cause (a) an oxidative removal of organic impurities adsorbed on the surface and (b) a recrystallization/reconstruction of the surface. It is well-known that an electrochemical pretreatment of gold by potential cycling leads to an activation of the electrode surface, e.g., for electrode processes such as the ORR [17]. The ORR responses of these two surfaces show that the $E_{1/2}$ of ORR of the electrochemically pretreated surface (150 cycles) is shifted by 0.170 V to more positive potentials than that of the as-polished surface (Fig. 1b). A similar shift of the peak potential by cycling was obtained on a glassy carbon electrode with immobilized AuNPs (curves not shown; see also part (B)). The theoretical ORR current is calculated from irreversible Randles-Ševčík equation (Eq. 1) [18].

$$i_{\text{peak}} = -0.496\sqrt{\alpha n' n} F A [O_2]_{\text{bulk}} \sqrt{\frac{F\nu D}{RT}} \quad (1)$$

where A is the geometric area of the gold or GC electrode (0.0314 cm^2), α is the transfer coefficient which is assumed to be 0.5, n' is the number of electrons involved in the rate

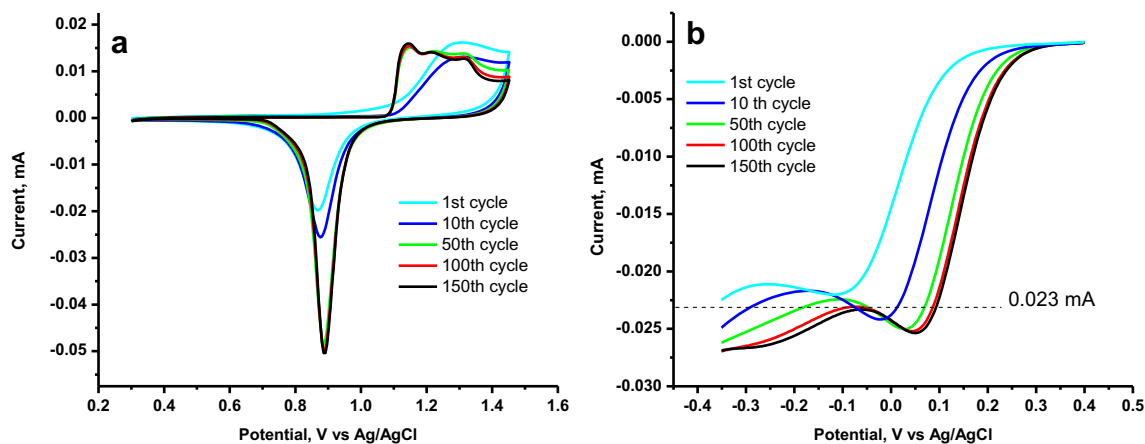


Fig. 1 **a** Cyclic voltammograms of a pc-Au electrode (geometric area of the electrode is 0.0314 cm^2): 1st cycle to 150th cycle and **b** their respective linear sweep voltammetric response of the oxygen reduction

reaction in oxygen-saturated 0.1 M sulfuric acid at a scan rate of 0.1 V s^{-1} (dotted line refers to the theoretically calculated current from the irreversible Randles-Ševčík equation)

determining step, here it is 1 as one-electron reduction of O_2 to superoxide radical anion is rate determining step, $n=2$ is the number of electron involved during the reduction of O_2 to peroxide, F is the Faraday constant, $[\text{O}_2]_{\text{bulk}}$ is the saturation concentration of dissolved oxygen ($1.26 \times 10^{-3} \text{ M}$) [19], D is the diffusion coefficient of O_2 ($1.93 \times 10^{-5} \text{ cm}^2 \text{ s}^{-1}$) [19], and v is the scan rate. The ORR current on the as-polished electrode is very close to the current calculated from irreversible Randles-Ševčík equation. However, the ORR current is slightly increasing with increasing number of electrochemical cycles. AFM showed that the electrode surface is also slightly roughening during electrochemical cycling. Though not so efficient, the electrochemical pretreatment also enhances the ability of the electrode to reduce hydrogen peroxide, an intermediate in the ORR. This can be deduced from the appearance of a second reduction wave between -0.1 and -0.35 V . The current of this second peak increase with increase in the number of electrochemical cycles.

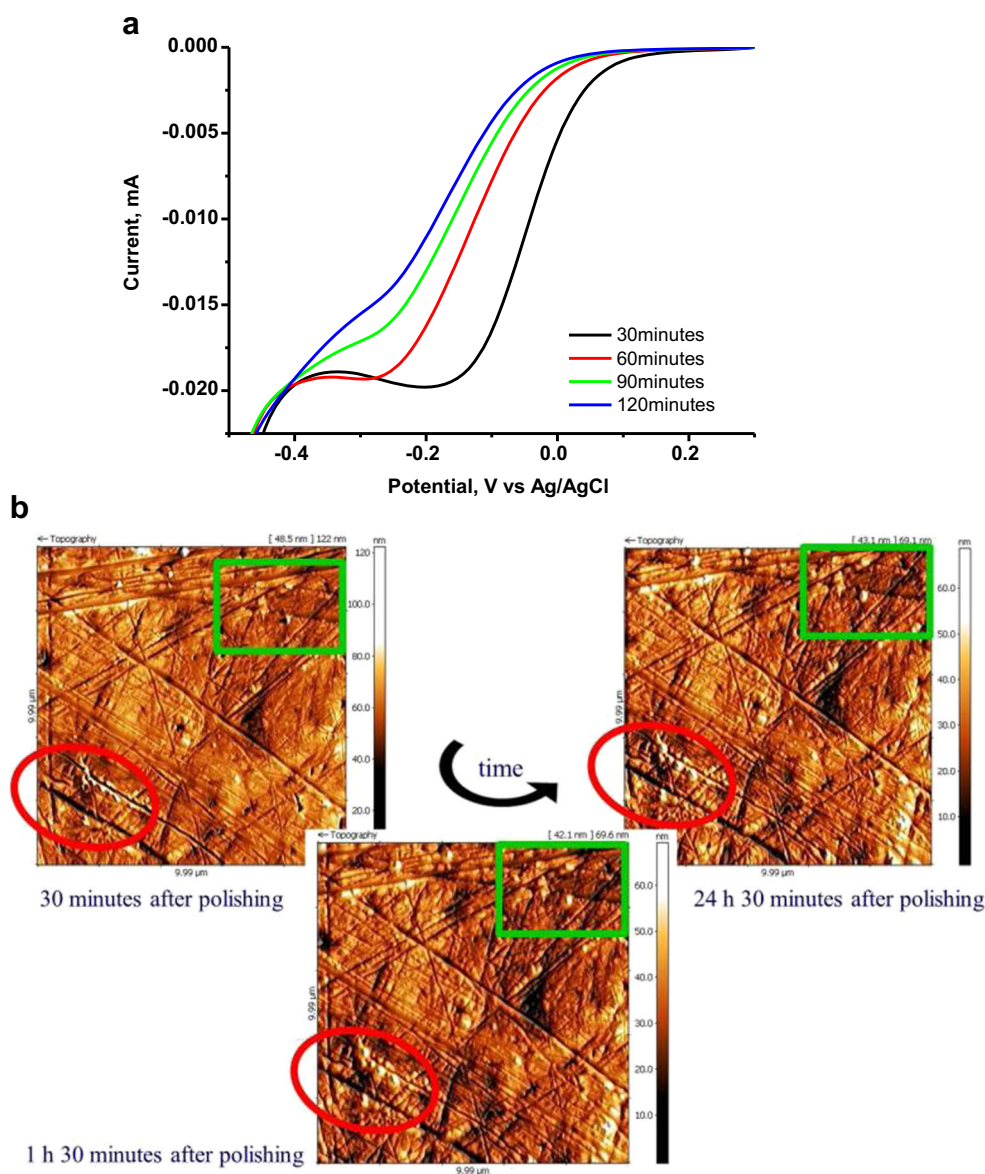
It is a well-known phenomenon that a high energy surface can relax to its original state (or lower energy state) by oxidation or reconstruction processes [20]. The ORR curves were recorded at the as-polished surface and then after different relaxation times (electrode again maintained under argon). The deactivation of the surface was evident from the observation of a negative shift of $E_{1/2}$ of the ORR curves with time. Figure 2a shows the linear sweep voltammograms of the ORR on a gold electrode with the time of relaxation after each electrochemical measurement, and the following features can be noted: (i) the ORR current does not vary very much, while (ii) the position of the signal strongly shifts to more negative potentials. This is very similar to what has been observed during the deactivation of a mechanically polished electrode by hydroxyl radicals [11]. The slight decrease in current with time can be attributed to the increased irreversibility of the ORR on the deactivating surface. The deactivation is associated with minute changes of the surface as revealed by

identical location AFM images indicating some recrystallization of the surface (Fig. 2b). A very similar behavior was observed after activation of the gold electrode with a very rough abrasive paper with relaxation periods up to 3 h (results not shown).

It was also observed that electrochemical cycling in *alkaline* solution (0.5 M NaOH) leads to an activation of the surface with heavy surface wrinkling. Electrochemical activation was performed by potential cycling between -0.75 V and $+0.75 \text{ V}$ vs. Ag/AgCl for 3000 cycles at a scan rate of 1 V s^{-1} followed by reduction at -0.5 V for 5 min. Figure 3a shows the ORR curves corresponding to the activated gold electrode with respect to relaxation time (electrode was kept under argon). As in the case of pc-Au electrodes activated in acidic media, also after activation in alkaline solution, the half-wave potential of the ORR is shifting to negative potentials with relaxation time. A unique observation was made when the activated pc-Au electrode was etched in a KCN/O_2 solution: the dissolution of the surface layer led to a strongly deactivated electrode in the ORR measurements (cf. Fig. 3b). Additionally, the exposure of the etched surface to argon does not affect the position of the ORR curve.

It is known that the asperities created on the surface of gold electrodes by mechanical polishing are necessary in catalyzing the ORR. At the microscopic level, the pc-Au surface can be viewed as a surface with many nano-scale asperities. These asperities are activated during the potential cycling in acidic and alkaline media and we have observed the $E_{1/2}$ of the ORR on these activated surfaces at ca. 0.15 and 0.1 V , respectively. The deactivation of these activated electrodes is noticed as the $E_{1/2}$ was shifted to ca. -0.15 and -0.12 V , respectively, after 120 min of the relaxation time (under argon). This is most probably due to the recrystallization of the surface in the relaxation process. The removal of active atoms on the surface of gold by KCN/O_2 etching strongly deactivates the surface for the ORR. In comparison with the hydroxyl radical attack

Fig. 2 **a** Linear sweep voltammograms of the oxygen reduction reaction on pc-Au electrode (polished with 50 nm alumina powder followed by ultrasonic cleaning for 2 min) in 0.1 M sulphuric acid at a scan rate of 0.1 V s^{-1} . *Time in minutes* indicates the exposure of the electrode to argon atmosphere in a desiccator after each electrochemical measurement. **b** Identical-location AFM topographical image of polished gold surface after 30 min, 1 h, and 30 min, and 24 h and 30 min exposure in ambient environment (the *rectangle* and *ellipse* highlight the areas with distinct changes in surface morphology)



on the gold surface, the removal of gold by cyanide etching removes a much thicker surface layer, and leaves a surface which is unaffected by mechanical machining and a build-up of the grain surface planes of polycrystalline gold. These experiments show that such surfaces do not give any electrocatalytic ORR response in the accessible potential range.

(B) Oxygen reduction reaction on AuNP-modified glassy carbon electrodes

Oxygen reduction experiments were performed with different amounts of AuNPs immobilized on a glassy carbon (GC) electrode. Immobilization of different amounts of AuNPs was considered as a way to introduce different amounts of asperities on the GC electrode. Figure 4 shows the cyclic voltammograms of the GC-AuNP electrodes: The well-

known gold oxide system increases in magnitude with increasing loads of AuNPs. Before measuring the ORR response, the GC-AuNP electrode was electrochemically pretreated by 50 potential cycles between 0.3 and 1.45 V at 0.1 V s^{-1} scan rate until a stable gold response was obtained. The monolayer oxidation features of AuNPs show two clearly visible peaks which are also present in the curves recorded with the pc-Au electrodes, where three peaks appear. This shows that the surface structure of AuNPs is different from that of pc-Au. There is also a small reduction shoulder after the main reduction peak, which is attributed to the gold dissolution and redeposition in the presence of trace amount of complexing chloride ions. From the charge of gold oxide reduction, the electrochemical surface area (ECSA) was calculated [21] assuming $390 \mu\text{C cm}^{-2}$ as the charge related to one monolayer of gold oxide reduction. Then, the roughness

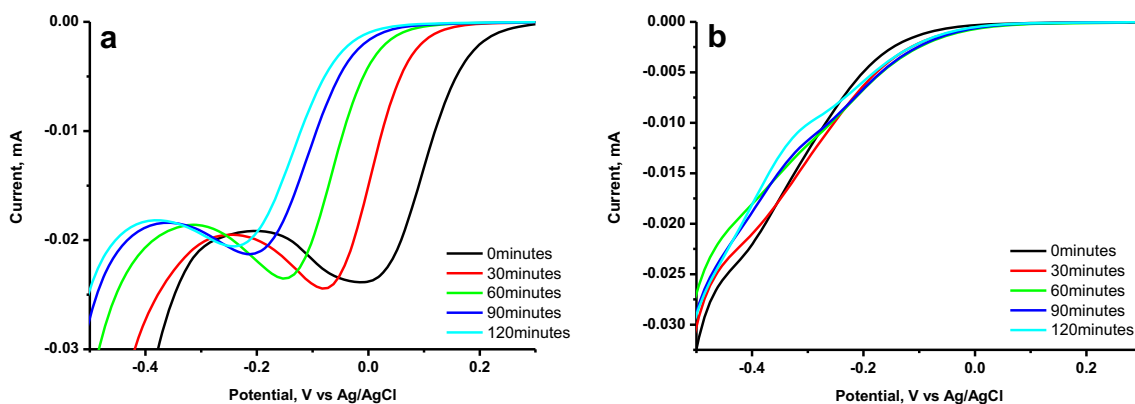


Fig. 3 Linear sweep voltammograms of oxygen reduction on **a** electrochemically activated gold electrode, **b** KCN/O₂-etched gold (1 % KCN; etching time: ca. 10 min) in oxygen-saturated 0.1 M

sulfuric acid at a scan rate of 0.1 V s⁻¹. *Time in minutes* indicates the exposure of the electrodes to argon after each electrochemical measurement in both **a** and **b**

factor (Ψ) was calculated from ECSA and the geometric surface area of the GC disc (0.0314 cm²).

Figure 5 depicts the ORR response of electrodes with increasing quantities of AuNPs: (i) the ORR current increases (5a), but it is not proportional to the active area (5b shows the current density with respect to ECSA); (ii) the potential shift of the ORR is significant; and (iii) when the surface reaches the maximum AuNP coverage, the ORR signal does not change. It was also observed that increasing the AuNP loading leads to the appearance of a second wave with increasing intensity in current and shifting of the peak position, similar to that observed when increasing the number of potential cycles using a pc-Au electrode. This wave was shown to be due to the reduction of hydrogen peroxide formed in the first wave of oxygen reduction. The second wave was missing at lower AuNP coverage, probably because of a more negative

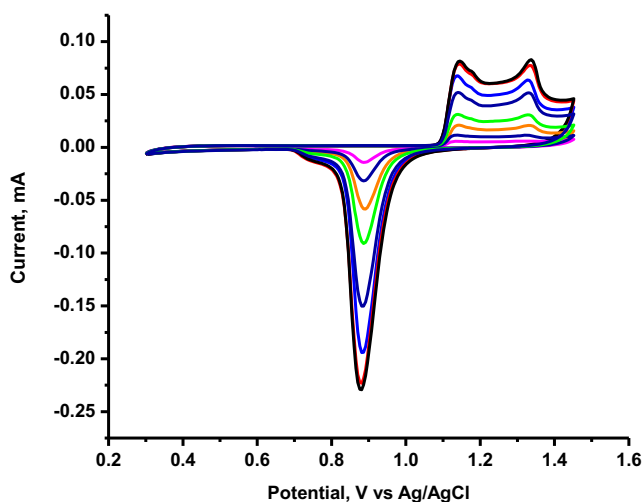


Fig. 4 Cyclic voltammograms of GC electrodes with increasing amounts of AuNPs sol on the surface in 0.1 M H₂SO₄. The scan rate of the sweep was 0.1 V s⁻¹. The roughness factor (Ψ) of gold: from magenta to black curves 0.9, 2.2, 4.2, 6.6, 11.1, 14.1, 17.3, and 18

position of the reduction wave of H₂O₂ (see upcoming section, Fig. 6a). It should be noted that hydrogen evolution takes place just below ca. -0.4 V on the AuNP-covered GC electrodes, which obscures hydrogen peroxide reduction. The calculated current for the ORR using the irreversible Randles-Ševčík equation (and the geometric surface area of the electrode used) was 0.023 mA, assuming a transfer coefficient of 0.5. When we compare the experimentally measured currents, it is clear that at higher coverages, the current exceeds this limit. It is important to note here that the current is not proportional to the real surface area, since the mass transport obeys semi-infinite linear diffusion, and changes in coverage and in turn of the real surface area are irrelevant for the current. To check the increased current, we formally calculated the transfer coefficient of ORR on AuNPs with the roughness factor of 2.2, 4.2, and 6.6 at 0.61, 0.67, and 0.76, respectively. Increase of transfer coefficient value with coverage favors the reduction of oxygen to hydrogen peroxide, and thus higher currents result. It is clear that the higher the electrochemical surface area or roughness, the higher is the amount of active sites, which may increase catalytic activity.

To verify whether the AuNP loading indeed catalyzes hydrogen peroxide reduction, we studied the reduction of H₂O₂ in deaerated electrolyte solutions of 3 mM H₂O₂. The voltammograms indeed indicate an increasing catalytic activity for hydrogen peroxide reduction to water, i.e., a shift in peak position to positive potentials (Fig. 6a). As the $E_{1/2}$ for O₂ and H₂O₂ reduction changes with the electrode loading of AuNPs, the shift may be interpreted as a consequence of changing reaction kinetics. To test this hypothesis, we used a cyclic voltammogram starting at 0.4 V going to negative potentials to first reduce oxygen to only hydrogen peroxide and the potential was then reversed to 1.1 V to oxidize the in situ-generated hydrogen peroxide (Fig. 6b). As expected, the peak separation (ΔE_p) between oxygen reduction and hydrogen peroxide oxidation was lowered with increased AuNP loading.

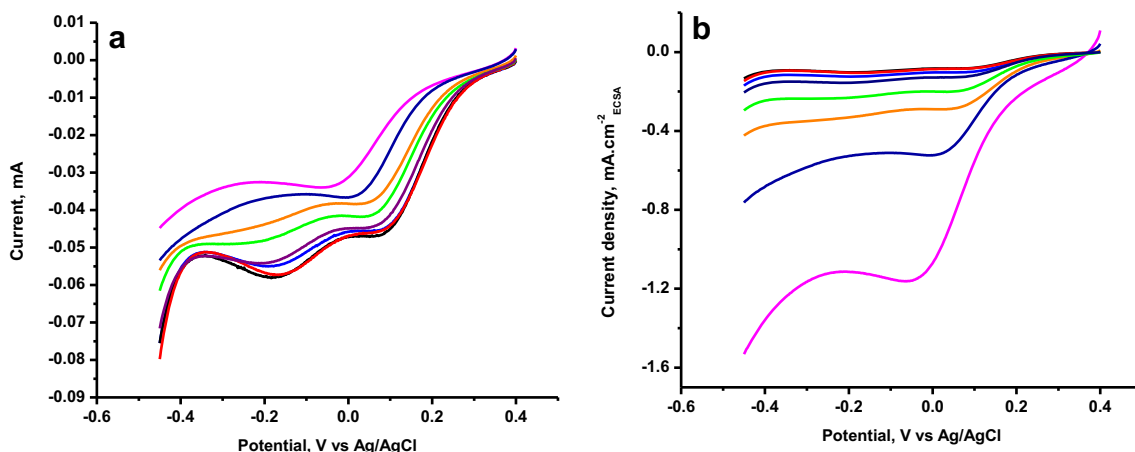


Fig. 5 Linear sweep voltammograms of oxygen reduction **a** in current, **b** in current density on AuNPs/GC electrode with varying coverages of AuNPs in oxygen-saturated 0.1 M sulfuric acid at a scan rate of 0.1 V s^{-1} .

The roughness factor (Ψ): from magenta to black curves 0.9, 2.2, 4.2, 6.6, 11.1, 14.1, 17.3, and 18

There are several interpretations of the observed shift of potential based on the geometric and electronic effects. In the case of electrocatalysis on gold, the surface structure of the nanoparticle seems to have a significant role in determining the activity. A concise account of the electrocatalysis of organic molecules oxidation and oxygen reduction on gold, which are sensitive to pH and surface structure has been recently reviewed by Koper et al [22]. Experiments and theoretical studies [23] showed that (100) single crystal faces or nanoparticles populated with (100) domains have higher oxygen reduction reaction reactivity than that of (111) and (110) in both acidic [24] and alkaline medium [25–27]. According to Nørskov et al. [28], band broadening and consequent *d*-band shift takes place due to the metal coordination number on the surface, which is a descriptor for the activity of many surface-specific reactions proved by theory and experiments. In our case, as we use AuNPs with a diameter of around 22 nm, which mostly behave like pc-Au, it may not have

significant electronic effect due to metal coordination on the observed positive potential shift. Ohsaka et al. [29] electrochemically deposited different amounts of gold on a GC surface and observed a shift of potential to positive values in neutral 0.1 M phosphate buffered saline (PBS) buffer. They explained the potential shift as being due to energy savings for the production of hydrogen peroxide. However, the physical reason for such change-over in catalysis is not explained. Jena and Raj have shown that the shift of peak potential of ORR with coverage of gold particles can be attributed to changes in the diffusion regime from mixed spherical to linear diffusion [12]. The explanation is based on the fact that the AuNPs cast on the electrode behave like an array of microelectrodes changing to macroelectrode-like behavior at higher coverage of nanoparticles. However, in practice, the immobilization of particles on the electrode surface may not form a perfect micro-electrode array, but instead form fractal aggregates with narrow inter-particle distances during evaporation [30, 31] or

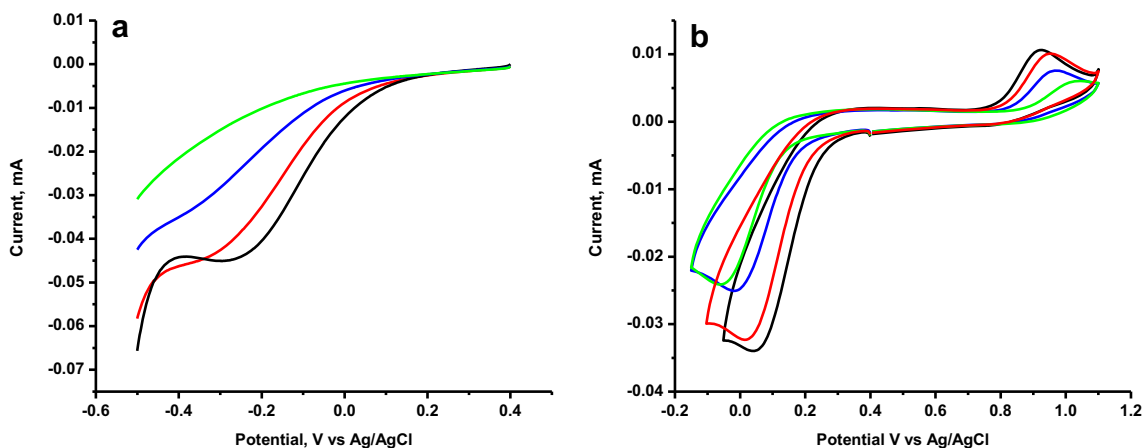


Fig. 6 **a** Linear sweep voltammograms of H_2O_2 reduction on electrochemically cleaned AuNPs/GC electrode with varying coverages of AuNPs in deaerated 0.1 M H_2SO_4 with 3 mM H_2O_2 at a scan rate of 0.1 V s^{-1} . **b** Cyclic voltammograms of oxygen reduction and oxidation of

oxygen reduction intermediate (H_2O_2) on electrochemically cleaned AuNPs/GC electrode with varying coverages of AuNPs in oxygen-saturated 0.1 M sulfuric acid at a scan rate of 0.1 V s^{-1} . The roughness factor (Ψ) of gold, from green to black curves is 0.9, 2.2, 4.2, and 6.6

under electrochemical reductive polarization conditions [32]. Figure 7(a-d) shows the SEM-EDX mapping of AuNPs with different coverages. From this figure, it is clear that increasing the AuNPs load leads to an increase of particle clustering, and increase of surface concentration of AuNP clusters.

Compton et al. ascribed these changes in activity based on the electrochemical surface area of array of particles with overlapped electric double layers (EDLs). In their papers [13, 14], they simulated the irreversible response of an electrocatalyzed system on spherical particles. They arrived at the following equation describing the shift of the peak potential to positive values with increasing coverage (Eq. 2):

$$E_{\text{peak}} = E_c^\ominus - \frac{RT}{\alpha F} \left[0.78 - \ln k_{\text{app}}^0 + \ln \left(\sqrt{\frac{\alpha F D \nu}{RT}} \right) \right] \quad (2)$$

where k_{app}^0 is the apparent rate constant, which is given by,

$$k_{\text{app}}^0 = \Psi k^0 \quad (3)$$

where k^0 is the true rate constant and Ψ is the ratio of surface area of electroactive particles to the geometric area of substrate.

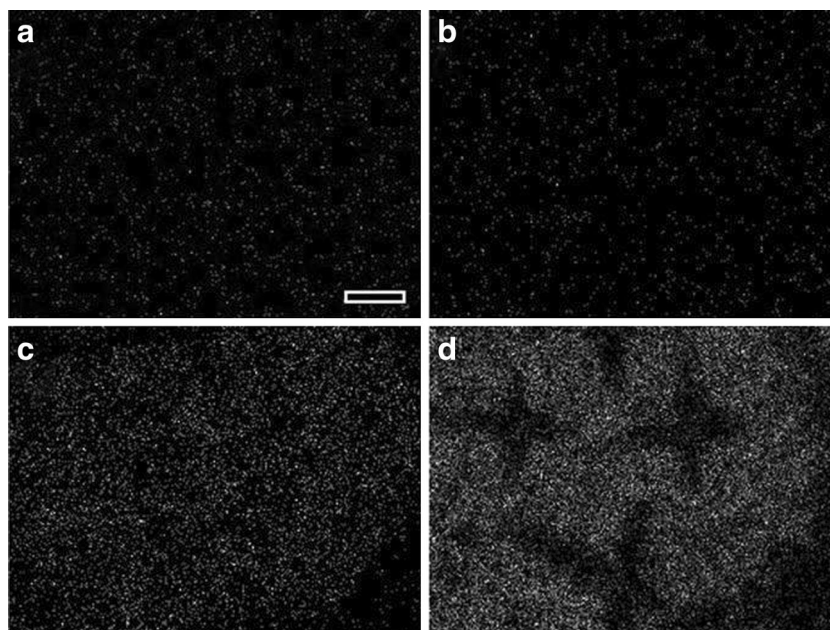
Equation 2 results from the assumption that the scale of the roughness of the surface is smaller than the scale of the diffusion layer thickness, and the assumption that the diffusion fields of neighboring electroactive regions strongly overlap so that the diffusion to the entire surface is linear. This analysis completely describes the experimental results. However, in a recent paper, Nesselberger et al. [15] have demonstrated that the inter-particle distance between platinum nanoparticles,

which are placed at a distance less than the Debye length, affects the activity by changing the compact layer potential (particle proximity effect). It is explained that the EDLs of individual nanoparticles overlap and increase the potential of the compact layer in a particle. As a result, the potential drop changes from top to bottom of the nanoparticles. They put forward the idea that the enhanced activity is due to the overlap of EDLs and a consequent potential drop and they defined the average compact layer potential as a descriptor for the activity by performing theoretical simulations and validated the results by experiments. Thus, it cannot be excluded that there is a real increase in the rate constant caused by this effect also in the case of gold nanoparticles. We suppose this double layer effect is also operative in the case of the AuNP-modified GC electrode. This may well account for potential shift. The increased coverage with AuNPs brings the particles closer together during evaporation or under electrochemical conditioning, leading to a marked clustering of the AuNPs. When the coverage of particles increases, the effect of overlap of the EDLs will proportionally affect the position of the current-potential curves as a result of changed kinetics. When the surface of GC is completely covered with particles, the lower layers of particles will not contribute much to electrochemistry because they are screened by a potential gradient (pore effect), and oxygen diffusion to the lower layers will also be strongly diminished. Therefore, it is understandable, that the effect levels off when multilayers of AuNPs are deposited.

Conclusion

The activation of pc-Au electrodes as well as experiments with GC electrodes modified with an increasing load of

Fig. 7 SEM-EDX mapping of gold-covered surface by drop cast of gold sol in micro liter: **a** 4, **b** 6, **c** 14, and **d** 20 μl corresponding to the roughness factor of 4.2, 6.6, 11.1, and 18 (scale bar=20 μm in **a** is applicable to all the images)



AuNPs clearly show that the current is only slightly affected by the number of active sites, but the potential is strongly shifted to positive potentials. The behavior exactly resembles that which Compton et al. [14] have simulated for electrodes with a varying surface coverage of electroactive sites, for sub-monolayer loading. We suggest that the shift of potential is the result of an increased clustering of nanoparticles and overlapping of the electrical double layers. Future studies should be directed on a quantitative analysis of experimental data so that a decision can be made, what is an apparent increase of the rate constant due to electrode surface geometry, and what is the possible contribution of the particle proximity effect proposed by Nesselberger et al. [15]. The deactivation of the electrode surface is highly dependent on the nature of surface asperities. Changes in the quality of the gold surface due to relaxation/reordering of the surface or the removal of the active sites detrimentally affect the activity.

Acknowledgments We acknowledge the support by Gregor Jatzlauk, who has recorded a number of AFM images, and the kind help of Nanjie Hu (Institute of Geology, University of Greifswald) for recording the SEM images.

References

1. L'Her M (2006) Electrochemistry of oxygen. In: Bard AJ, Stratmann M, Scholz F, Pickett JC (eds) Encyclopedia of electrochemistry, inorganic electrochemistry. Wiley-VCH, Weinheim
2. Katsounaros I, Cherevko S, Zeradjanin AR, Mayrhofer KJJ (2014) *Angew Chem Int Ed* 53:102–121
3. Appleby A, Zagal J (2011) *J Solid State Electrochem* 15:1811–1832
4. Burke LD, Hurley LM (1999) *Electrochim Acta* 44:3451–3473
5. Burke LD, Hurley LM (2000) *J Solid State Electrochem* 4:353–362
6. Burke LD, Hurley LM, Lodge VE, Mooney MB (2001) *J Solid State Electrochem* 5:250–260
7. Cherevko S, Kulyk N, Chung C-H (2012) *Electrochim Acta* 69:190–196
8. Burke LD, O'Mullane AP (2000) *J Solid State Electrochem* 4:285–297
9. Burke LD, Casey JK, Morrissey JA (1993) *Electrochim Acta* 38:897–906
10. Burke LD, Nagle LC (1999) *J Electroanal Chem* 461:52–64
11. Nowicka AM, Hasse U, Sievers G, Donten M, Stojek Z, Fletcher S, Scholz F (2010) *Angew Chem Int Ed* 49:3006–3009
12. Jena BK, Raj CR (2007) *Langmuir* 23:4064–4070
13. Gara M, Ward KR, Compton RG (2013) *Nanoscale* 5:7304–7311
14. Ward KR, Gara M, Lawrence NS, Hartshorne RS, Compton RG (2013) *J Electroanal Chem* 695:1–9
15. Nesselberger M, Roefzaad M, Fayçal Hamou R, Ulrich Biedermann P, Schweinberger FF, Kunz S, Schloegl K, Wiberg GKH, Ashton S, Heiz U, Mayrhofer KJJ, Arenz M (2013) *Nat Mater* 12:919–924
16. Polte J, Ahner TT, Delissen F, Sokolov S, Emmerling F, Thunemann AF, Kraehnert R (2010) *J Am Chem Soc* 132:1296–1301
17. Wang Y, Laborda E, Crossley A, Compton RG (2013) *Phys Chem Chem Phys* 15:3133–3136
18. Nicholson RS, Shain R (1964) *Anal Chem* 36:706–723
19. Stamenković V, Schmidt TJ, Ross PN, Marković NM (2002) *J Phys Chem B* 106:11970–11979
20. Binder K, Bowker M, Inglesfield JE, Rous PJ (1995) *Cohesion and structure of surfaces*. Science, Elsevier
21. Trasatti S, Petrii OA (1992) *J Electroanal Chem* 327:353–376
22. Rodriguez P, Koper MTM (2014) *Phys Chem Chem Phys* 16:13583–13594
23. Viswanathan V, Hansen HA, Rossmeis J, Nørskov JK (2012) *J Phys Chem Lett* 3:2948–2951
24. Alvarez-Rizatti M, Jüttner K (1983) *J Electroanal Chem Interfacial Electrochem* 144:351–363
25. Hernández J, Solla-Gullón J, Herrero E (2004) *J Electroanal Chem* 574:185–196
26. Hernández J, Solla-Gullón J, Herrero E, Aldaz A, Feliu JM (2007) *J Phys Chem C* 111:14078–14083
27. El-Deab MS, Sotomura T, Ohsaka T (2005) *Electrochem Commun* 7:29–34
28. Nørskov JK, Abild-Pedersen F, Studt F, Bligaard T (2011) *Proc Natl Acad Sci* 108:937–943
29. El-Deab MS, Okajima T, Ohsaka T (2003) *J Electrochem Soc* 150:A851–A857
30. Lin MY, Lindsay HM, Weitz DA, Ball RC, Klein R, Meakin P (1989) *Nature* 339:360–362
31. Manthiram K, Surendranath Y, Alivisatos AP (2014) *J Am Chem Soc* 136:7237–7240
32. Toh HS, Batchelor-McAuley C, Tschulik K, Uhlemann M, Crossley A, Compton RG (2013) *Nanoscale* 5:4884–4893